Arch. Metall. Mater. **68** (2023), 4, 1497-1502

DOI: https://doi.org/10.24425/amm.2023.146215

F. KAMIL[1], I. HAMISAH[1], M. HASMALIZA[1*]

MECHANICAL PROPERTIES OF BIOACTIVE GLASS-CORDIERITE COMPOSITE

Bioactive glass (BG) can be utilized as a replacement and regeneration material for orthopaedic and orthodontic. However, a load-bearing structure requires good mechanical properties to withstand high stress, in addition to good bioactivity properties. In this research, BG and cordierite (BG-cord) composite was fabricated to improve BG's mechanical properties. The mechanical strength of the BG-cord was investigated. Both BG and cordierite were synthesized separately using the glass melting method. The synthesized BG and cordierite powders were used to fabricate BG-cord using a composition variation from 10 to 50 wt.%. The composite with 30 wt.% cordierite demonstrated the highest diametral tensile strength (DTS), 14.01 MPa.

Keywords: Bioactive glass; cordierite; tensile mechanical

1. Introduction

Bioactive glass (BG) is among the preferred materials for clinical treatment applications, particularly in the orthopaedic [1] and orthodontic disciplines [2]. In recent years, the demand for BG escalates, corresponding to the rise in the human population and bone defects regeneration [3-5]. The outstanding properties of BG that make it unique among other materials are excellent osteoconductivity and bioactivity [6], drug delivery [7], good ability to deliver cells [8], and controllable biodegradability [9]. As an implant, BG exercises the ability to strongly bond an artificial material with living tissues such as bone through the emergence of a crystalline apatite layer with biological activity with identical properties to bone mineral, making it able to integrate with the host bone [10]. The formation of a strong bond between the implant material and bone results from apatite crystallization of the implant material surface in reacting with body fluid solutions [11]. The presence of silica-hydroxyl rich layer (Si-OH) groups on the implant material and the dissolution of calcium and phosphate ions from BG contribute significantly to apatite crystallization [12]. Moreover, a layer rich in amorphous $CaO\text{-}P_2O_5$ is formed on the silica-hydroxyl-rich layer, crystallising and forming an apatite layer [3].

However, based on previous research, BG demonstrates low mechanical properties and brittle behavior very fragile and prone to catastrophic failure, rendering it unsuitable for load-bearing applications [13,14]. It also possesses lower fracture toughness and elastic modulus compared to the human cortical bone [15]. Because of these reasons, failure of a BG implant may occur through fracture at the BG-bone interface during the implantation itself. An exciting approach to solving this issue is incorporating cordierite into BG to form a composite that BG reinforced with cordierite to improve strength and performance.

The ceramic material of choice, cordierite, is a suitable crystalline ceramic material of the $MgO\text{-}Al_2O_3\text{-}SiO_2$ ternary system with good chemical resistance and mechanical properties (~243 MPa) [16]. Mengucci et al. utilized cordierite as a biomaterial in the form of a sintered honeycomb monolith. In order to enhance the mechanical resistance, insolubility, chemical resistance, and porosity of cells, cell growth can be regarded as the best option in addition to its low production costs [17]. Krajewski et al. demonstrated that cordierite could promote cell growth effectively [18]. The chemical ion of Mg^{2+} in cordierite composition could encourage cell attachment through a positive effect between the ceramic surface electrostatic charge and the potential cell membrane [19]. Furthermore, magnesium ions are in the cordierite structure, an essential trace element in the human body. In bone growth and regeneration, magnesium has been shown to perform a significant role and provide great osteoconductivity over time [20].

Additionally, no research has been performed on BG and cordierite composite. Several materials were nevertheless used

[1] UNIVERSITI SAINS MALAYSIA, SCHOOL OF MATERIALS AND MINERAL RESOURCES ENGINEERING,BIOMATERIAL RESEARCH NICHE GROUP, 14300 NIBONG TEBAL, PENANG, MALAYSIA

* Corresponding author: hasmaliza@usm.my

as a composite to enhance BG properties. Fortunately, BG was also used to boost the bioactivity of inert materials such as metal since it has a strong bioactivity efficiency [21-23]. Polymer materials were also used to develop BG-polymer composites because the polymer cannot easily bind to living tissues on its own; however, at the same time, the polymer has strong flexibility characteristics. It can be biodegraded in the replacement of soft tissues [24-26]. Inert materials such as alumina and zirconia also develop as a composite with BG due to their antifriction properties, and high strength was significantly ideal for determining femur heads and ceramic inserts (acetabular cups) in hip joint prostheses. The BG and inert ceramic composite have normally been manufactured to make the inert material bioactive. The composite has been developed for biomedical use to improve bond strength in bone formation and accelerate the recovery period compared to inert material monolith [27]. Also, the BG composite has been developed with other bioactive ceramics such as hydroxyapatite. Devis Belucci et al. formed BG-HA composites developed in which the composite increased the crystallization so that higher temperatures could be sintered to achieve higher mechanical strength [28]. Karajian et al. also investigate the positive response of BG-calcium phosphate composites to encourage the osteogenic differentiation of the cell population and enhance BG's mechanical strength [29]. In general, that was important to design the composite development of BG.

Therefore, cordierite into BG is expected to enhance its mechanical properties, which is the mechanical properties of a ceramic composite material relying on various parameters. The composition amount of materials is among the important parameters influencing the overall composite properties. This research aims to study the influence of cordierite powder composition in bioactive glass-cordierite composite (BG-cord) to enhance the mechanical properties of bioactive glass.

2. Materials and method

2.1. Sample preparation

2.1.1. Synthesis of 45S5 BG and cordierite

Both BG and cordierite were synthesized using the glass melting method. The 45S5 bioactive glass composition (45 SiO_2 – 24.5 CaO – 24.5 NaO – 6 P_2O_5 in wt.%) was used in the synthesis. High purity silicon dioxide (SiO_2) (99.5%, Ipoh Ceramic, Malaysia), phosphorus pentoxide (P_2O_5) (99%, Fluka, Italy), calcium carbonate ($CaCO_3$) (99.95%, Merck, United States), and sodium carbonate (Na_2CO_3) (99.9%, Merck, United States) powders were mixed for 24 hours in a polyethylene (PE) bottle at 25 rpm. The mixed raw material powder was then melted for an hour in the alumina crucible for the temperature at 1400°C before quenching using distilled water as media. Subsequently, the glass frit obtained after quenching was dried, then milled for one hour to produce fine BG powder. The cordierite (53 SiO_2 – 26 Al_2O_3 – 21 MgO in wt.%) was synthesized using a mixture of aluminum dioxide (Al_2O_3) (99.5%, Fluka, Italy), magnesium oxide (MgO) (98%, Qrec, New Zealand), and silicon dioxide (SiO_2) (99.5%, Ipoh Ceramic, Malaysia) powders. All the raw materials were homogenously mixed for 24 hours in a PE bottle by rolling at 25 rpm. The raw material mixture was melted for 4 hours at 1550°C in the alumina crucible before quenching it in distilled water. To obtain cordierite glass powder, the collected frit was dried, then milled for 15 minutes. The glass powder was subsequently calcined to form crystalline cordierite at 980°C for soaking time 2 hours. The cordierite was milled for an additional 3 hours.

2.1.2. Fabrication of BG-cord

Synthesized BG and cordierite powders obtained were mixed at variable compositions in PE bottles for 6 hours at 25 rpm. The mixture of powders was compacted to cylinder shape with 13 mm diameter using a hydraulic press at 650 MPa before sintering at 600°C. The different compositions of BG and cordierite used in this research study are tabulated in TABLE 1.

TABLE 1

Composition of BG and cordierite in weight percentage (wt.%) of BG-cord

Sample	Composition (wt.%)	
	BG	Cordierite
BG-10%cord	90	10
BG-20%cord	80	20
BG-30%cord	70	30
BG-40%cord	60	40
BG-50%cord	50	50

2.2. Characterization

2.2.1. Particle size analysis

Prior to the BG-cord composite fabrication, the particle size of both BG and cordierite was evaluated by analyzing the milled BG and cordierite using a dry particle size analyzer (Sympatec, Helos, England).

2.2.2. Porosity

The porosity of samples was measured using the Archimedes principle method. The samples were immersed in distilled water, and the apparent weight loss in the Archimedes Buoyancy is equal to the weight of the displaced fluid. The sample was placed in the desiccator for 1 hour in distilled water and vacuum to ensure that the water filled the pores and all the bulbs left the sample. The dry sample was weighed (*Md*) sample was then placed in the beaker to be put on the nylon chain (*Ms*) as it was

being measured; the samples were hanged in water (*Ms*), where the density of water, ρ = 1 g/cm^3. Sample and weight (*Mw*) were cleaned. Eq. (1) was used to measure density. Bulk density and porosity equations are described in Eqs. (1) and (2).

$$\text{Bulk density} = \frac{Md}{Mw - Ms} \times \rho\,\text{water} \tag{1}$$

$$\text{Apparent porosity} = \frac{Mw - Md}{Mw - Ms} \times 100\% \tag{2}$$

2.2.3. Diametral tensile strength (DTS)

Mechanical properties of BG-cord were determined by diametral tensile strength (DTS) test (Instron 3367, America) at a crosshead speed of 0.5 mm/min with 5 kN load based on the ASTM-D3967. The calculation of DTS was present in formula (3), where *P* = Force was applied. *D* = diameter of the sample, *T* = thickness of the samples, π = constant, 3.142.

$$DTS = \frac{2P}{\pi DT} \tag{3}$$

2.2.4. Hardness

The Vickers hardness test was performed. In order to make a measured indentation, the Vickers hardness test uses 3 kN loads and 10 seconds dwell time. Before the testing, the samples were ground using sandpaper and then polished to obtain a smooth surface. The smooth surface samples were placed on the Vickers hardness machine. The Vickers hardness of BG-cord was calculated using Eq. (4), and the schematic diagram was shown in Fig. 1.

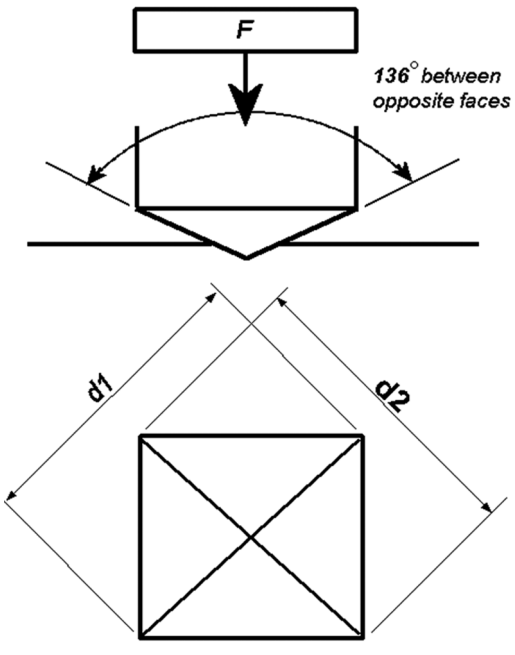

Fig. 1. Vickers hardness schematic diagram

$$HV = 0.102 \frac{2F \sin\frac{136°}{2}}{d^2} \tag{4}$$

F – Load applied (kN),
d^2 – Mean of diagonal of the indentation (mm).

3. Results and Discussion

3.1. Particle size analysis

Before the BG-cord composite fabrication, the particle size of the BG and cordierite powders was analyzed. The particle size distribution graph is presented in Fig. 2. Fig. 2 shows the most considerable and median particle size analyzed of BG and cordierite powder after milling were tabulated in TABLE 3. The particle size distributions analysis of both BG and cordierite is portrayed in Fig. 2, where BG was found to have a smaller particle size than cordierite. This is because of the composition disparity between BG and cordierite with amorphous and crystalline (orthorhombic) atomic structures, respectively [30]. A material with an amorphous structure is more accessible to crush than the one with a crystalline structure since the atoms in an amorphous structure are more likely to slide when a force is applied during milling than a packed and arranged atomic structure, which is much harder to crush.

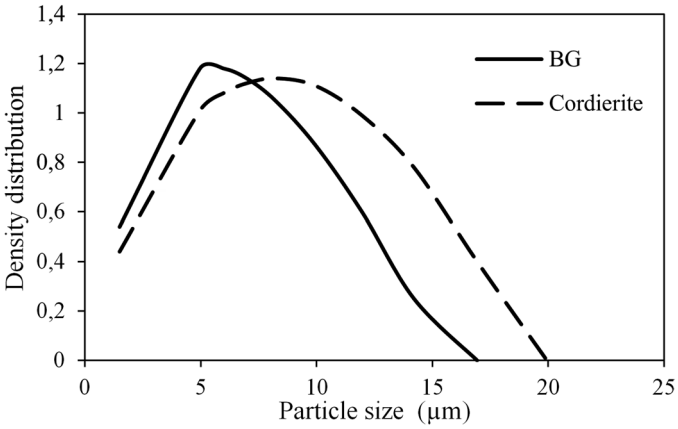

Fig. 2. Distribution of particle size BG and cordierite powder after milling

TABLE 3 illustrates that both BG and cordierite powders' particle sizes are smaller than 38 μm at D_{100}, significant in bioactive function. Smaller particle size promotes the higher specific

TABLE 3

Largest and median particle size of BG and cordierite particle after milling

Powder	Largest particle size, D_{100} (μm)	Median particle size, D_{50} (μm)
BG	16.93	4.35
Cordierite	19.94	5.45

surface area, promoting accelerating ion diffusion due to the quick dissolution of ions such as Si^{4+} and Ca^{2+}, which impacts the bioactivity performance degree at the implant interface. Furthermore, materials with a particle size smaller than 38 μm are required for cell culture mediation as cells sizes are often in the range of 4-40 μm [31].

3.2. X-ray diffraction analysis (XRD)

After the BG and cordierite were milled, the BG-cord was fabricated. The XRD analysis was done to determine the phase present of monolith BG and BG-cord. The results of the XRD analysis for all samples are shown in Fig. 3.

The XRD analysis revealed that the monolith BG possesses an amorphous structure with a significant combeite crystal phase, $Na_6Ca_3Si_6O_{18}$, (ICDD No.: 98-002-1442). An amorphous glass is formed upon fast cooling during a quenching process below the glass's transition temperature [10]. In a melting process, the atoms in a molten glass move randomly and are immediately fixed but with irregular arrangement upon quenching. This phenomenon is due to the insufficient time for the atoms to rearrange within the sample. The combeite phase started to appear when the atoms in the monolith BG pellets began to crystallize at 600°C upon sintering. Combeite provides essential properties that could enhance a material or composite's bioactivity [32] and mechanical properties [33]. Similar combeite and cordierite (ICDD No.:98-001-7002) were observed for all BG-cord samples of various cordierite compositions. Besides, the intensity of cordierite peak in the XRD spectra increases simultaneously with the increasing concentration of cordierite in the composite, where the BG-50%. Cord sample showed the highest peak intensity due to the highest amount of cordierite used. On the other hand, the quantity and intensity of the combeite phase peak decrease when a higher amount of cordierite is incorporated in the composite.

3.3. Porosity

The porosity conditions of the monolith BG and the fabricated BG-cord composite was presented in Fig. 4. Based on Fig. 4, the porosity of BG increases with the increasing composition of cordierite. This occurs due to the difference in particle size between BG and cordierite particles, where the cordierite powder has a larger particle size than BG particles, as shown in TABLE 2. The larger particle size reduces the contact area between BG and cordierite particle size, thus creating more hollow parts (pores) and increasing the porosity [34]. The composite's porosity increased gradually due to the increasing number of pores when the cordierite composition was increased.

3.4. Diametral tensile strength (DTS)

The DTS of the various BG-cord compositions was evaluated, and the correlations between DTS and porosity for all composite samples are displayed in Fig. 5. Based on Fig. 5, cordierite increases BG DTS when up to 30 wt.% was added into the BG composition. The DTS value increases with the increasing amount of cordierite in the BG-cord composite, where a maximum DTS value of 14.01 MPa was achieved when 30 wt.% cordierite was added, which was higher compared to monolith BG (6.29 MPa).

Fig. 5 also illustrates that the BG-cord composites' porosities (16.63% to 31.52%) are higher than that of the monolith BG (12.66%), which simultaneously resulted in the higher DTS values of the BG-cord composites. This shows the critical role of cordierite in strengthening BG rather than the compacting effect. However, the DTS value decreases, starting from 40 wt.% of cordierite addition due to porosity. A higher porosity in the sample results in more hollow spaces thus reduces the obstacle to withstand the force applied.

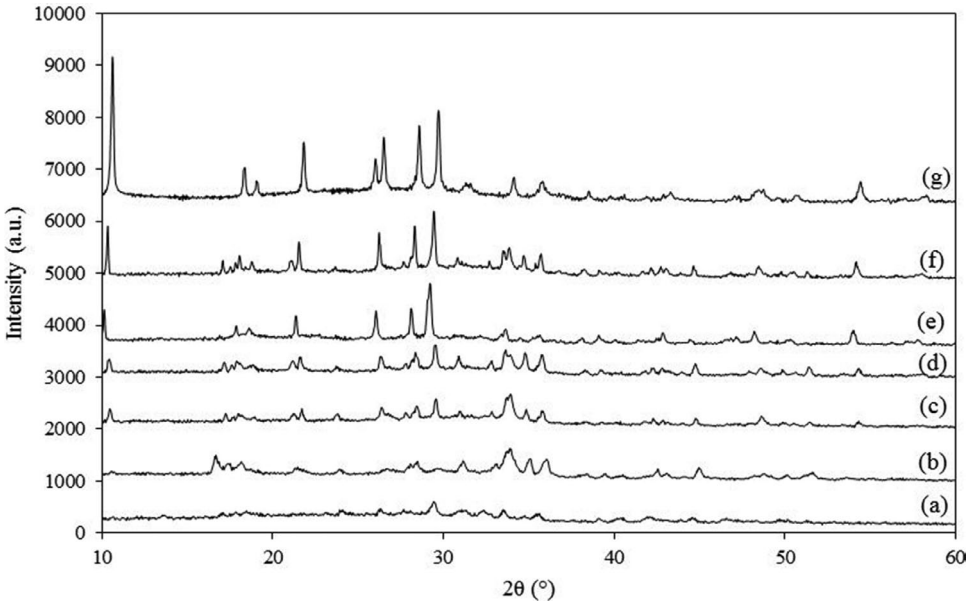

Fig. 3. XRD analysis of: (a) BG, (b) BG-10%cord, (c) BG-20%cord, (d) BG-30%cord, (e) BG-40%cord, (f) BG-50%cord, (g) Cordierite

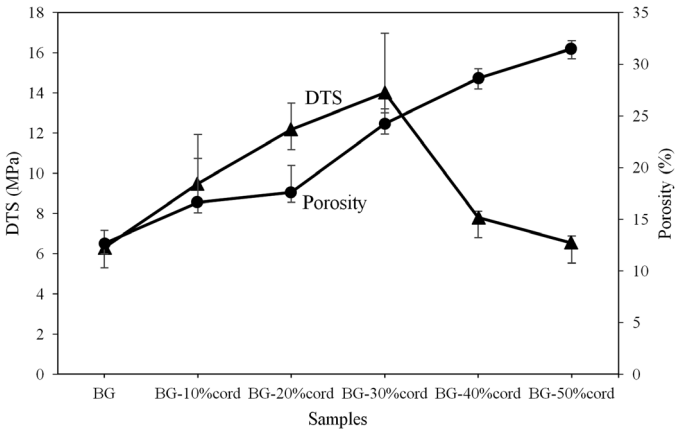

Fig. 5. DTS and porosity of monolith BG and BG-cord with the variation of the composition

3.5. Hardness

The physical properties of monolith BG and BG-cord with different compositions were measured using the hardness test. The hardness for all samples is presented in Fig. 6. Based on Fig. 6, BG-cord's hardness decreased compared to monolith BG from 147 Hv to 113.87 Hv for BG-10%. Cord and the hardness keep decreased to 24.5 Hv when the composition of cordierite increases. This is due to the increase of porosity of the sample, which is porosity influenced the hardness of ceramic bodies [35].

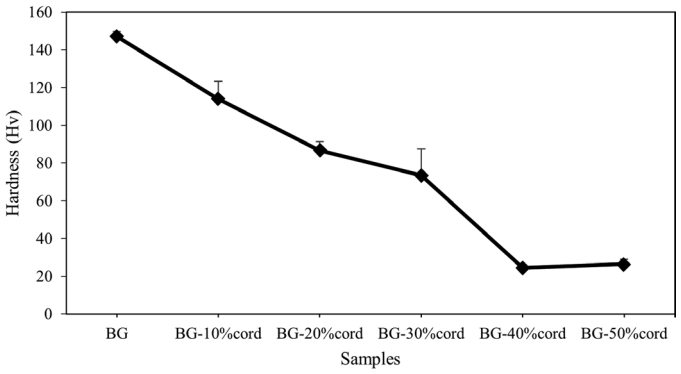

Fig. 6. Hardness of the monolith BG and BG-cord with the variation of the composition

4. Conclusion

BG-cord composite was successfully fabricated by experimenting with a variation of BG and cordierite compositions. An improvement in the BG-cord composites' mechanical properties was observed with high DTS values when cordierite was incorporated. Overall, the BG-cord composite with 30 wt.% cordierite (BG-30%cord) demonstrated the highest DTS value of 12.35 Mpa and hardness of 73.37 Hv with 24.24% porosity.

Acknowledgement

The authors would also like to extend their recognition to the Ministry of Higher Education Malaysia for Fundamental Research Grant Scheme (FRGS) with Project Code : FRGS/1/2019/TK05/USM/02/6.

REFERENCES

[1] L. Hench, Chronology of bioactive glass development and clinical applications, New J. Glas. Ceram. **2013**, 67-73 (2013). Accessed: Dec. 01, 2016. [Online]. DOI: http://file.scirp.org/Html/2-1030072_30885.htm

[2] D. Bellucci, R. Salvatori, J. Giannatiempo, A. Anesi, S. Bortolini, V. Cannillo, A new bioactive glass/collagen hybrid composite for applications in dentistry, Materials (Basel), **12**, 13, 2-7 (2019). DOI: https://doi.org/10.3390/ma12132079

[3] J.R. Jones, Review of bioactive glass: from Hench to hybrids, Acta Biomater. **9**, 1, 4457-86, Jan. (2013). DOI: https://doi.org/10.1016/j.actbio.2012.08.023

[4] F. Baino, S. Hamzehlou, S. Kargozar, Bioactive glasses: Where are we and where are we going?, J. Funct. Biomater. **9**, 1 (2018). DOI: https://doi.org/10.3390/jfb9010025

[5] Z. Goudarzi, N. Parvin, F. Sharifianjazi, Formation of hydroxyapatite on surface of SiO2–P2O5–CaO–SrO–ZnO bioactive glass synthesized through sol-gel route, Ceram. Int. **45**, 15, 19323-19330 (2019). DOI: https://doi.org/10.1016/j.ceramint.2019.06.183

[6] A. Ardeshirylajimi et al., Enhanced osteoconductivity of polyethersulphone nanofibres loaded with bioactive glass nanoparticles in in vitro and in vivo models, Cell Prolif. **48**, 4, 455-464 (2015). DOI: https://doi.org/10.1111/cpr.12198

[7] W. Hong et al., Roles of strontium and hierarchy structure on the in vitro biological response and drug release mechanism of the strontium-substituted bioactive glass microspheres, Mater. Sci. Eng. C **107**, July 2019, 110336 (2020). DOI: https://doi.org/10.1016/j.msec.2019.110336

[8] Y. Zhang, J. Luan, S. Jiang, X. Zhou, M. Li, The effect of amino-functionalized mesoporous bioactive glass on MC3T3-E1 cells in vitro stimulation, Compos. Part B Eng. **172**, no. January, 397-405 (2019). DOI: https://doi.org/10.1016/j.compositesb.2019.05.104

[9] Q.Z. Chen, I.D. Thompson, A.R. Boccaccini, 45S5 Bioglass®-derived glass – ceramic scaffolds for bone tissue engineering, Biomaterials **27**, 11, 2414-2425 (2006). DOI: https://doi.org/10.1016/j.biomaterials.2005.11.025

[10] N. Farhana, H. Mohamad, S. Noor, F. Mohd, N. Ahmad, Apatite formation on melt-derived bioactive glass powder based, Ceram. Int. **43**, 15, 11676-11685 (2017). DOI: https://doi.org/10.1016/j.ceramint.2017.05.356

[11] D.C. Clupper, J.J. Mecholsky, G.P. LaTorre, D.C. Greenspan, Bioactivity of tape cast and sintered bioactive glass-ceramic in simulated body fluid, Biomaterials **23**, 12, 2599-2606, Jun. (2002). DOI: https://doi.org/10.1016/S0142-9612(01)00398-2

[12] B. Zagrajczuk, M. Dziadek, Z. Olejniczak, K. Cholewa-kowalska, M. Laczka, Structural and chemical investigation of the

gel-derived bioactive materials, Ceram. Int. **43**, no. May, 12742-12754 (2017).
DOI: https://doi.org/10.1016/j.ceramint.2017.06.160

[13] D. Bellucci, A. Sola, L. Lusvarghi, V. Cannillo, Ceram. Int. **40**, 3805-3808 (2014).
DOI: https://doi.org/10.1016/j.ceramint.2013.08.018

[14] G. Yang, X. Yang, L Zhang, M. Lin, X. Sun, X. Chen, Z. Gou, Mater. Lett.**75**, 80-83 (2012).
DOI: https://doi.org/10.1016/j.matlet.2012.01.122

[15] T. Kokubo, H.M. Kim, M. Kawashita, Biomaterials **24**, 2161-2175 (2003). DOI: https://doi.org/10.1016/S0142-9612(03)00044-9

[16] M.M.S. Sanad, M.M. Rashad, E.S.A. Abdel-Aal, M.F. El-Shahat, K.W. Powers, Int. J. Appl. Ceram. Technol. **11**, 864-871 (2014).
DOI: https://doi.org/10.1111/ijac.12237

[17] P. Mengucci, G. Majni, A. De Benedittis, G. Biagini, Biomaterials **19**, 1447-1450 (1998).

[18] A. Krajewski, A. Ravagliolo, M. Kirsch, G. Biagini, R. Solmi, M. Belmonte, C. Zucchini, M.G. Gandolfi, C. Castaldini, L. Rodriguez, R. Giardino, R. Mongiorgi, E. Roncari, L. Orlandi. J. Mater. Sci. Mater. Med. **7**, 99-102 (1996).
DOI: https://doi.org/10.1007/BF00058720

[19] L. Orlandi, R. Solmi, A. Krajew, A. Bearzatto, G. Biaginig, E. Ciccopiedil, A. Ravaglioli, Biomaterials **18**, 955-961 (1997).

[20] J. Ma, C.Z. Chen, D.G. Wang, J.H. Hu, Ceram. Int. **37**, 1637-1644 (2011). DOI: https://doi.org/10.1016/j.ceramint.2011.01.043

[21] N.M.S. Adzali, S.B. Jamaludin, M.N. Derman, Rev. Adv. Mater. Sci. **30**, 262-266 (2012).

[22] Z.M. Al-Rashidy, M.M. Farag, N.A. Abdel Ghany, A.M. Ibrahim, W.I. Abdel-Fattah, Surf. Coatings Technol. **334**, 479-490 (2018).
DOI: https://doi.org/10.1016/j.surfcoat.2017.11.052

[23] A. Sola, D. Bellucci, V. Cannillo, A. Cattini, Surf. Eng. **27**, 560-572 (2011). DOI: https://doi.org/10.1179/1743294410Y.0000000008

[24] S. Srinivasan, R. Jayasree, K.P. Chennazhi, S.V. Nair, R. Jayakumar, Carbohydr. Polym. **87**, 274-283 (2012).
DOI: https://doi.org/10.1016/j.carbpol.2011.07.058

[25] K.M.J. Aitasalo, J.M. Piitulainen, J. Rekola, P.K. Vallittu, Head Neck **36**, 1391 (2014). DOI: https://doi.org/10.1002/HED

[26] A.R. Boccaccini, M. Erol, W.J. Stark, D. Mohn, Z. Hong, J.F. Mano, Compos. Sci. Technol. **70**, 1764-1776 (2010).
DOI: https://doi.org/10.1016/j.compscitech.2010.06.002

[27] K. Zhang, Q. Van Le, J. Compos. Compd. **2**, 10-17 (2019).

[28] D. Bellucci, L. Desogus, S. Montinaro, R. Orrù, G. Cao, V. Cannillo, Innovative hydroxyapatite/bioactive glass composites processed by spark plasma sintering for bone tissue repair, J. Eur. Ceram. Soc. **37**, 4, 1723-1733 (2017).
DOI: https://doi.org/10.1016/j.jeurceramsoc.2016.11.012

[29] M. Karadjian et al., Biological properties of calcium phosphate bioactive glass composite bone substitutes: Current experimental evidence, Int. J. Mol. Sci. **20**, 2, 1-22 (2019).
DOI: https://doi.org/10.3390/ijms20020305

[30] K. Morinaga, H. Takebe, Phase Relations and Transformations in Advanced Ceramic Materials, High Temp. Mater. Process. **22**, 3-4, 141-150 (2003).
DOI: https://doi.org/10.1515/HTMP.2003.22.3-4.141

[31] N. Farhana, H. Mohamad, S. Noor, F. Mohd, Characterization on melt-derived bioactive glass powder from, J. Non-Crystalline Solids J. **462**, 23-31 (2017).
DOI: https://doi.org/10.1016/j.jnoncrysol.2017.01.040

[32] T.T. Swe, H. Mohamad, K.A. Shariff, A.A. Thant, Fabrication of sol-gel derived new quaternary silicate Bioglass S55P4, AIP Conf. Proc. **2068**, no. January, (2019).
DOI: https://doi.org/10.1063/1.5089369

[33] L.A. Adams, E.R. Essien, A.T. Adesalu, M.L. Julius, Bioactive glass 45S5 from diatom biosilica, J. Sci. Adv. Mater. Devices **2**, 4, 476-482 (2017). DOI: https://doi.org/10.1016/j.jsamd.2017.09.002

[34] M. Rahimian, N. Ehsani, N. Parvin, H. Reza Baharvandi, The effect of particle size, sintering temperature and sintering time on the properties of Al-Al2O3 composites, made by powder metallurgy, J. Mater. Process. Technol. **209**, 14, 5387-5393 (2009).
DOI: https://doi.org/10.1016/j.jmatprotec.2009.04.007

[35] Z. Balak, M. Zakeri, M.R. Rahimipur, E. Salahi, H. Nasiri, Effect of open porosity on fl exural strength and hardness of ZrB_2-based composites, Ceram. Int. **41**, 7, 8312-8319 (2015).
DOI: https://doi.org/10.1016/j.ceramint.2015.02.143